Microstructure and fracture behaviour of ZrO_2 (2 mol % Y_2O_3) reinforced with SiC whiskers

F. YE
State Key Laboratory of Solidification Processing, Northwestern Polytechnical University, Xi'an Shaanxi 710072, People's Republic of China

T. C. LEI, Y. C. ZHAO, Y. ZHOU
Department of Metals and Technology, Harbin Institute of Technology, Harbin 150001, People's Republic of China

The microstructure, mechanical properties, fracture behaviour and toughening mechanisms of 20 vol % SiC_w–ZrO_2 (2 mol % Y_2O_3) composite were investigated by X-ray diffraction, scanning and transmission electron microscopies, energy dispersive analysis of X-rays, high-resolution electron microscopy techniques and the three-point bending test. The results show that the ZrO_2 (2 mol % Y_2O_3) matrix is well strengthened and toughened by 20 vol % SiC_w. The SiC whiskers are directly bonded to the matrix with no interfacial reaction layer or amorphous phase. The main toughening mechanisms of the composite are crack deflection, dynamic tetragonal to monoclinic ZrO_2 transformation, whisker pull-out and crack bridging. In addition, the fracture behaviour of the composite was observed using an *in situ* fracture technique.

1. Introduction

ZrO_2 matrix ceramic is one of the main structural ceramics. Its fracture toughness has been improved remarkably by the tetragonal to monoclinic ($t \rightarrow m$) ZrO_2 transformation and microcrack toughening [1, 2]. However, the transformation effect disappears at temperatures higher than M_s.

Whisker reinforcement offers an effective toughening concept for monolithic structural ceramics [3–5]. In particular, SiC whiskers combine high strength and high elastic moduli with good thermal stability, and are the main reinforcements incorporated into ceramic matrices. Many investigators have reported that ceramic matrix composites reinforced with SiC whiskers have much higher toughness than that of the monolithic matrix, and the whisker toughening effect is not restricted by increasing temperature [6]. The effect of toughening (such as crack deflection, whisker pull-out and bridging) is sensitive to the microstructure of the composite, and in particular to the interfacial structure between whisker and matrix [4, 5, 7]. In this study, the microstructure and fracture behaviour of ZrO_2 (2 mol % Y_2O_3)–20 vol % SiC_w composite were investigated by means of X-ray diffraction (XRD), scanning and transmission electron microscopies (SEM), and high-resolution electron microscopy (HREM). Particular emphasis has been placed on studying in detail the toughening mechanisms using an *in situ* fracture technique.

2. Experimental procedure

The materials used in this study were a solid solution of ZrO_2 reinforced with 20 vol % SiC_w, and ZrO_2 powders were stabilized by 2 mol % Y_2O_3, with an average size of about 0.65 μm; the chemical compositions are shown in Table I. The whiskers (supplied by Toksi, Cabon, Japan) had a diameter of 0.1 μm and a length of 20–30 μm, and the mechanical properties are shown in Table II. The composites were hot-pressed at 1600 °C for 1 h under a pressure of 25 MPa.

Flexural strength and fracture toughness of the composites were measured in air at room temperature using an Instron 1186 machine. Flexural strength measurements were performed on bar specimens (3 mm × 4 mm × 36 mm) using a three-point bend fixture with a span of 30 mm. Fracture toughness measurements were performed on single-edge notched bar (SENB) specimens (2 mm × 4 mm × 25 mm) with a span of 16 mm, and a half-thickness notch was made using a diamond wafering blade.

TABLE I Chemical composition of ZrO_2 (2 mol % Y_2O_8) powder (wt %)

Material	ZrO_2	Al_2O_3	Y_2O_3	SiO_2	Fe_2O_3	NaO_2	CaO	MgO
ZrO_2 (2 mol % Y_2O_3)	96.36	< 0.02	3.6	< 0.017	< 0.01	< 0.01	< 0.01	< 0.01

0022–2461

Fracture surfaces of the composite were examined using a Hitachi S-570 scanning electron microscope. The microstructure of the composite was characterized by TEM. Thin-foil specimens, taken normal to the hot-pressing axis, were prepared by dimpling and subsequent ion-beam thinning. The whisker/matrix interface structures were examined in a JEM-2000EX-I high-resolution electron microscope at atomic-level resolution.

The size and the shape of the specimens for *in situ* SEM observations are shown in Fig. 1. The specimens were mounted in a fixture for *in situ* experiments in the scanning electron microscope with the polished side facing the electron beam for direct observation of the crack trace.

TABLE II The mechanical properties of β-SiC whisker

Material	D (kg m^{-2})	$\delta_{0.2}$ (MPa)	E (GPa)
β-SiC	3190	3–14	400–700

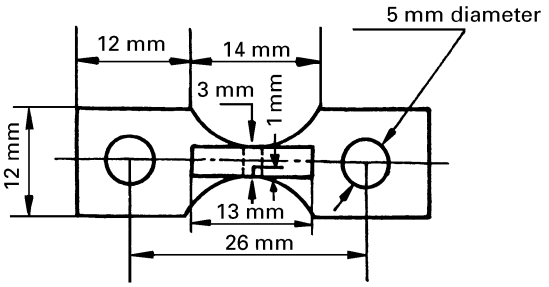

Figure 1 Tensile specimen for SEM *in situ* observation.

3. Results and discussion

3.1. Microstructure of 20 vol % SiC_w–ZrO_2 (2 mol % Y_2O_3) composite

Typical structures of the composite are shown in Fig. 2. The interfacial region in the matrix shows the lath structure of monoclinic phase ZrO_2 (2 mol % Y_2O_3) transformed by induction of residual thermal stress due to the difference in the thermal expansion coefficient between the whisker and matrix ($\alpha_{ZrO_2} = 10 \times 10^{-6}\,K^{-1}$, $\alpha_{SiC} = 5 \times 10^{-6}\,K^{-1}$). This t → m transformation could dissipate some of the interfacial residual stress and hence be of benefit to the properties of the composite [8]. The microcracks caused by the t → m ZrO_2 (2 mol % Y_2O_3) transformation can also be seen from Fig. 2. The microcracks also increase the toughness of the composite [3].

Interface characteristics of the composite are shown in Fig. 3, indicating that the whiskers have a good bond with the matrix grains. No interfacial reaction

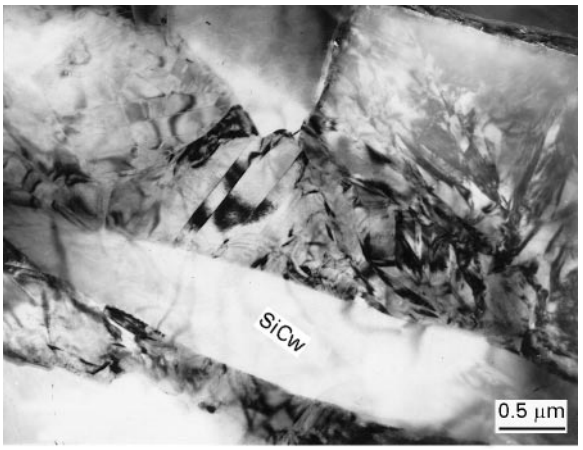

Figure 3 Transmission electron micrographs of the composite showing the lath structure of stress-induced monolinic phase in the matrix near the whisker/matrix interface.

Figure 2 Transmission electron micrographs of the ZrO_2 matrix in 20 vol % SiC_w–ZrO_2 (2 mol % Y_2O_3) composite showing microcracks induced by t → m ZrO_2 transformation.

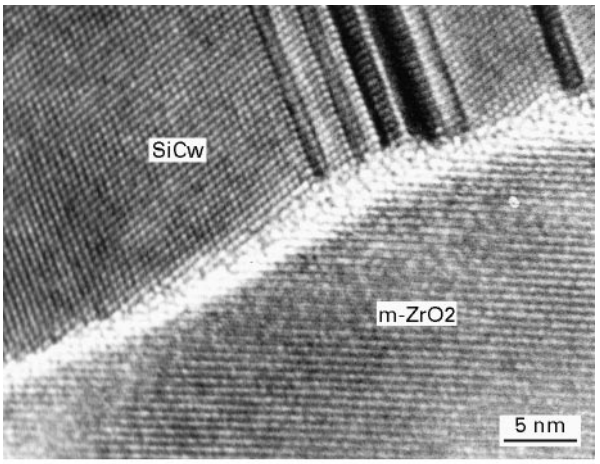

Figure 4 HREM image from SiC_w/ZrO_2 interface in the 20 vol % SiC_w–ZrO_2 (2 mol % Y_2O_3) composite indicating no reaction layer or amorphous phase at the interface between the whisker and matrix.

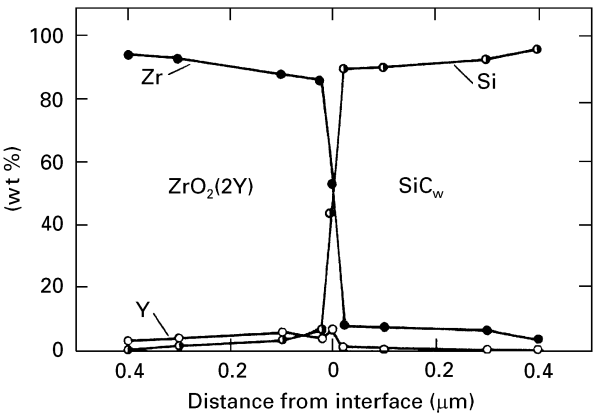

Figure 5 EDAX chemical analyses performed on the SiC/ZrO_2 interface.

TABLE III Room-temperature mechanical properties of ZrO_2 (2 mol % Y_2O_3) matrix and 20 vol % SiC_w–ZrO_2 (2 mol % Y_2O_3) composite

Materials	Flexural strength (MPa)	Fracture toughness (MPa $m^{1/2}$)
$ZrO_2(Y_2O_3)$	887 ± 70	13.71 ± 1.85
SiC_w–$ZrO_2(Y_2O_3)$	1341 ± 23	16.31 ± 1.06

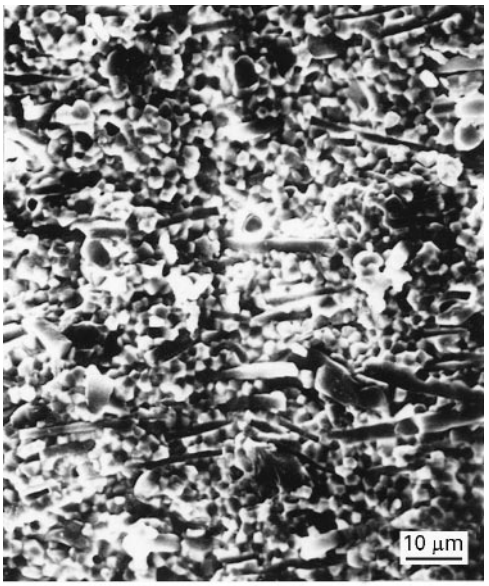

Figure 6 Fracture surfaces of SiC_w–ZrO_2 (2 mol % Y_2O_3) composite.

layer or amorphous phase exists at the interface. The t → m transformation due to the interfacial residual thermal stress during cooling at the end of fabrication, can also be seen clearly from Fig. 3. Fig. 4 shows

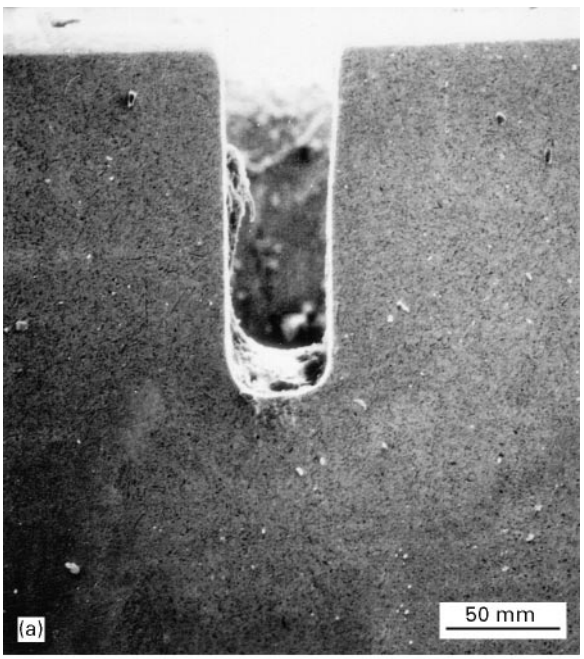

Figure 7 Scanning electron micrographs of the *in situ* tensile specimen of 20 vol % SiC_w–ZrO_2 (2 mol % Y_2O_3) composite, (a) before tension, (b) after tension showing the initiation of the crack at the notch.

a high-resolution electron micrograph of the interface between ZrO_2 and SiC whiskers. It demonstrates more clearly that the SiC whiskers are directly bonded to ZrO_2 crystals.

The results of EDAX chemical analyses performed on the interface between SiC whisker and matrix are shown in Fig. 5. The silicon content on the SiC side is over 93 wt % and there is little zirconium and yttrium due to the ion thinning, and in addition, the silicon content on the ZrO_2 side is less than 3 wt %, indicating no elemental diffusion between SiC_w and ZrO_2 at the interface, which is consistent with the results of TEM and HREM observations. The results of Yang and Steven's study on TZP/SiC system indicate that a glass phase existed at the interface associated with the presence of SiO_2 impurity present in the TZP matrix [3].

3.2. Mechanical properties of the composite

The mechanical properties of the SiC_w/ZrO_2 (2 mol % Y_2O_3) composite and the ZrO_2

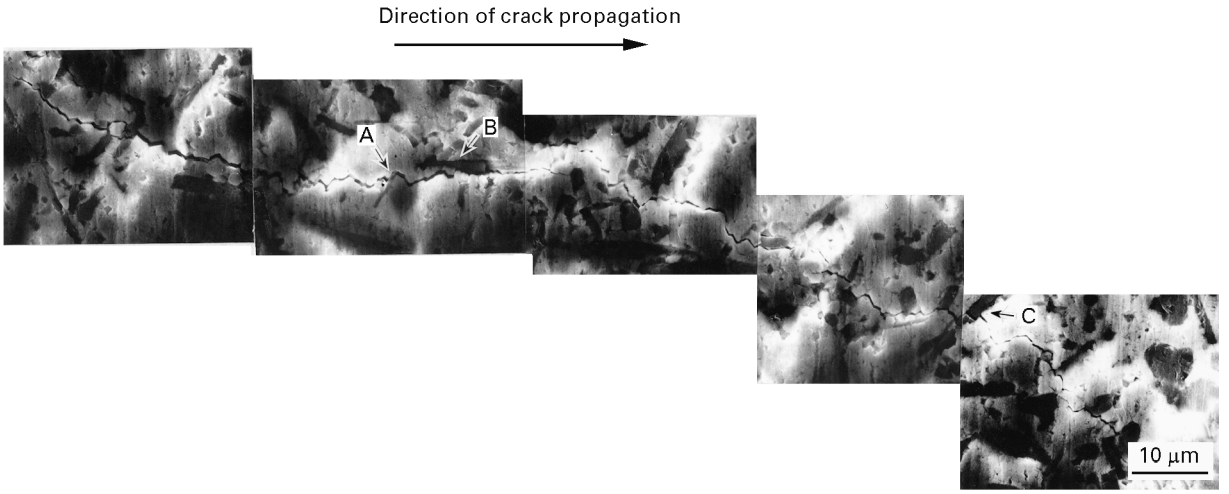

Figure 8 *In situ* scanning electron micrographs of crack propagation.

Figure 9 The late stage of the crack propagation shown in Fig. 8.

(2 mol % Y_2O_3) matrix are summarized in Table III. It can be seen that the composite shows an increase of 453 MPa in strength and 2.65 MPa $m^{1/2}$ in toughness compared to the ZrO_2 (2 mol % Y_2O_3) matrix, indicating that SiC whiskers incorporated into the ZrO_2 (2 mol % Y_2O_3) matrix provided good combined effects of strengthening and toughening.

The flexural fracture surface of the composite is shown in Fig. 6. It appeared to be quite rough with evidence of whisker pull-out, revealing substantial crack/microstructure interactions. Crack deflection and whisker pull-out undoubtedly make a contribution to the fracture toughness of the composite.

The XRD results indicate a considerable increase of the amount of m-ZrO_2 on the fractured surface in comparison to the polished surface caused by the dynamic t → m ZrO_2 phase transformation during the fracturing, which also makes a contribution to fracture toughness.

3.3. *In situ* SEM fracture observation of SiC_w/ZrO_2 composite

As stated above, the main toughening mechanisms of the composite are crack deflection, whisker bridging and pull-out, and dynamic t → m ZrO_2 phase transformation. The fracture behaviour of the composite can be demonstrated more clearly using *in situ* SEM observation.

Fig. 7 shows the initiation of a crack at the notch tip of the tensile specimen during the initial loading stage. With the increase in the applied load, the initial crack began to propagate (Fig. 8). Generally, the fracture followed an intergranular path in the ZrO_2 (2 mol % Y_2O_3) matrix with markedly abrupt deflections along or around the whiskers, although not always exactly along the whisker/matrix interfaces. This reveals a substantial amount of crack interaction with the microstructure. The bridging of the crack surfaces behind the crack tip by SiC whiskers can be seen clearly, and the width of the bridging zone is about 100 μm.

After continuous loading, the main crack proceeds further and bridging whiskers lose the bridging effect, as shown in Fig. 9, and which can be seen clearly from the higher magnification micrographs (Fig. 10). A new bridging region was formed behind the crack tip. It can be seen that the crack propagation paths have been strongly influenced by the whisker orientation to the proceeding crack plane (Figs 9 and 11). For the crack plane parallel to the whisker axis, the crack always propagates along the whisker/matrix interface (arrow B, Fig. 8). For the crack plane normal to the whisker axis, the whisker generally ruptures and the crack propagates across the whisker (arrow M, Fig. 9). For the crack plane inclined to the whisker, either the crack passes over the whisker (arrow A, Fig. 8, arrows L, I, J, Fig. 9) or the crack at first deflects along the whisker/matrix interface and then the whisker ruptures (arrow C, Fig. 8; arrow H, Fig. 9). Fig. 12 shows the *in situ* SEM observations of the composite after fracture, indicating whisker pull-out. The microcracks

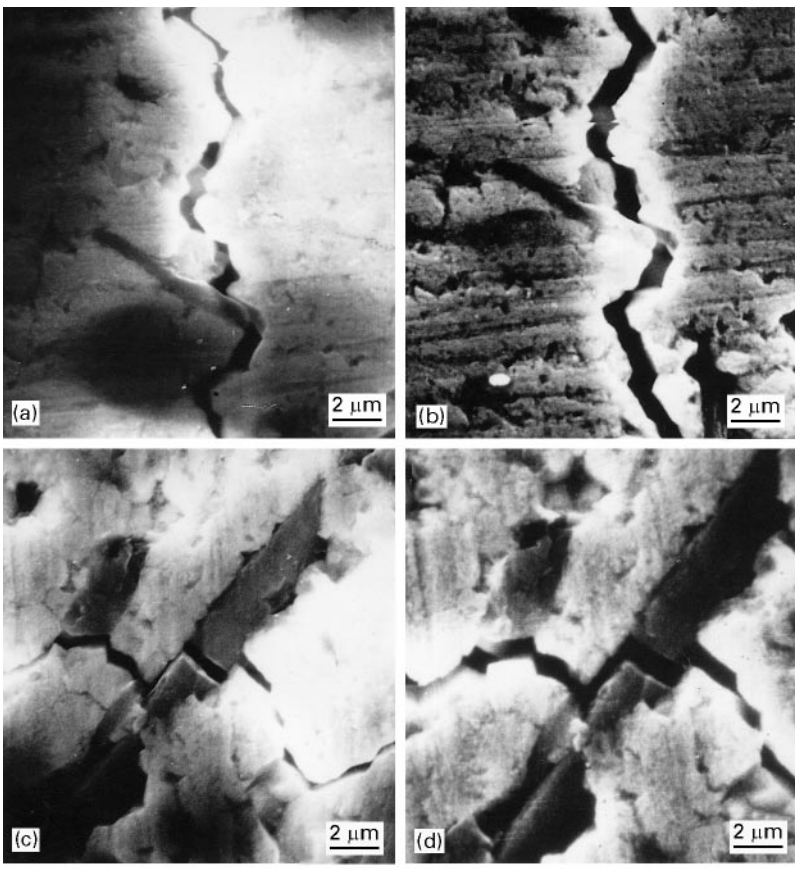

Figure 10 High-magnification images of some regions shown in Figs 8 and 9. (a, c) High-magnification images of regions A and C shown in Fig. 8, indicating crack bridging. (b, d) High-magnification images of regions E and G shown in Fig. 9, indicating the disappearance of crack bridging at a continuous loading.

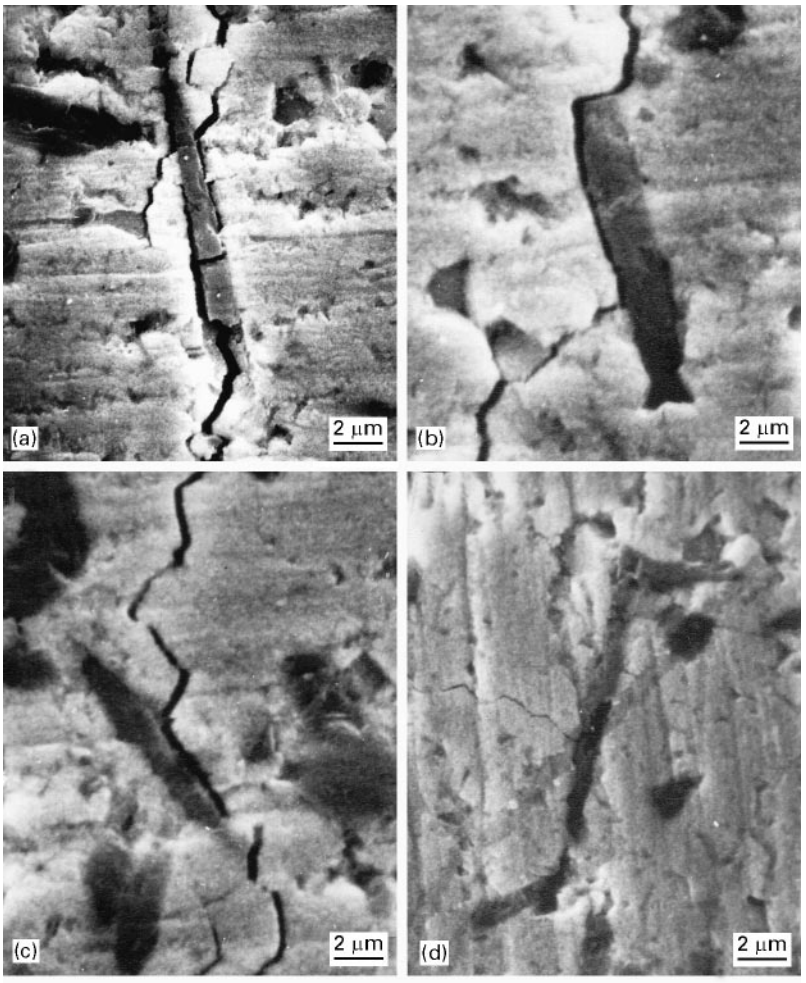

Figure 11 High-magnification images of some regions shown in Fig. 9. (a) High-magnification image of region H showing debonding of the whisker/matrix interface and crack deflection. (b, c) High-magnification images of regions I and J showing crack deflection. (d) High-magnification image of region K showing that the crack was restrained by a whisker.

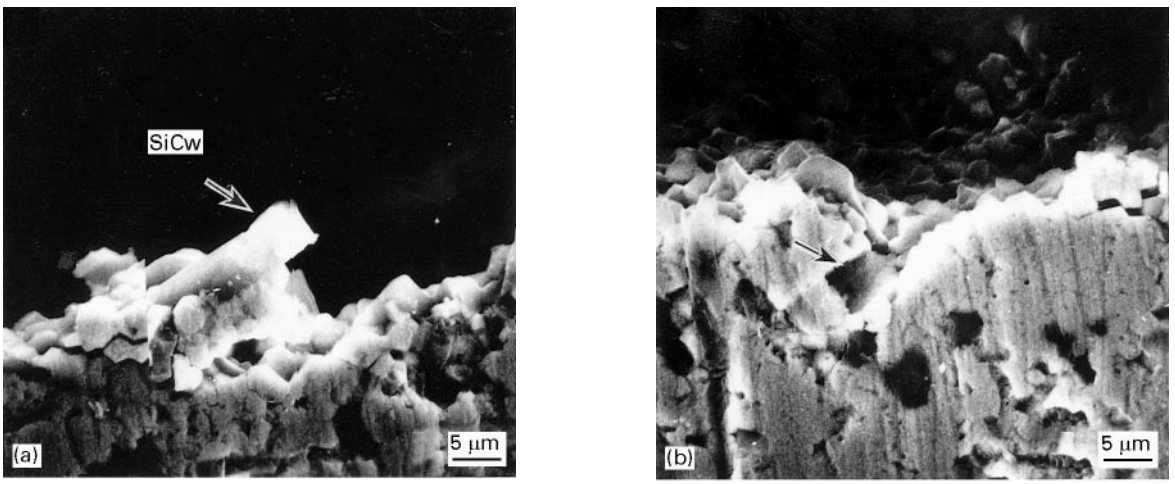

Figure 12 Scanning electron micrographs of the composite after fracture showing whisker pull-out: (a) the pulled-out whisker, (b) the residual hole caused by the whisker pull-out shown in (a).

due to the dynamic t → m ZrO_2 transformation can also be seen from Figs 8 and 9.

Becher *et al.* [9] and Homeny *et al.* [10] also reported that matrix cracks propagate past the whiskers and result in bridging whiskers in the wake of the crack tip. The observations also indicate that the development of interface cracks/debonding when the matrix crack reaches the interface, allows the matrix crack to proceed without fracturing the whisker. This will require that the interfacial fracture energy be much lower than that of the matrix or the whisker. An undulating interface or strong interfacial chemical bonding enhances the interface strength [11, 12]. Therefore, the fracture toughness of the composites could be further increased by the interface design.

4. Conclusions

1. The interface between β-SiC whiskers and the adjacent crystalline matrix grains of 20 vol % SiC_w–ZrO_2 (2 mol % Y_2O_3) composite did not, in general, contain thin amorphous films; the whiskers are directly bonded to the matrix crystals.

2. SiC whiskers incorporated into the ZrO_2 (2Y) matrix provided better combined effects of strengthening and toughening

3. *In situ* fracture observations clearly reveal that the main toughening mechanisms of the composite are crack deflection, whisker bridging and pull-out, and dynamic t → m ZrO_2 (2 mol % Y_2O_3) transformation.

References

1. R. M. McMEEKING and A. G. EVANS, *J. Amer. Ceram. Soc.* **65** (1982) 242.
2. A. G. EVANS and R. M. CANNON, *Acta Metall.* **34** (1986) 761.
3. M. YANG and R. STEVENS, *J. Mater. Sci.* **26** (1991) 726.
4. J. HOMENY and W. L. VAUGHN, *J. Amer. Ceram. Soc.* **73** (1990) 2060.
5. W. BRAUE, R. W. CARPENTER and D. J. SMITH, *J. Mater. Sci.* **25** (1990) 2949.
6. P. F. BECHER and T. N. TIEGS, *Adv. Ceram. Mater.* **3** (1988) 148.
7. J. J. BRENNAU and S. R. NUTT, *J. Amer. Ceram. Soc.* **75** (1992) 1205.
8. P. F. BECHER and T. N. TIEGS, *ibid.* **70** (1987) 651.
9. P. F. BECHER, C. H. HSUEH, P. ANGELINI and T. N. TIEGS, *ibid.* **71** (1988) 1050.
10. J. HOMENY, W. L. VAUGHN and M. K. FERBER, *Amer. Ceram. Soc. Bull.* **67** (1987) 233.
11. T. AKATSU, Y. TANABE, S. MATSNURA, M. YAMADA, H. ISHII, M. MUNAKATA and E. YASUDA, *J. Ceram. Soc. Jpn, Int. Edn* **99** (1991) 416.
12. G. A. HOLMQUIST and J. A. PASK, *J. Amer. Ceram. Soc.* **59** (1976) 384.

Received 19 January
and accepted 17 September 1996